Radio Astronomy at the Fringe
ASP Conference Series, Vol. 300, 2003
J.A. Zensus, M.H. Cohen, & E. Ros (eds.)

arXiv:astro-ph/0304164v2 6 May 2003

Variability and Velocity of Superluminal Sources

M. H. Cohen, M. A. Russo
Department of Astronomy, MS 105-24, California Institute of Technology, Pasadena, CA 91125, USA

D. C. Homan, K. I. Kellermann, M. L. Lister
National Radio Astronomy Observatory, 520 Edgemont Road, Charlottesville, VA 22903, USA

R. C. Vermeulen
Netherlands Foundation for Research in Astronomy, P.O. Box 2, NL-7990 AA Dwingeloo, The Netherlands

E. Ros, J. A. Zensus
Max-Planck-Institüt für Radioastronomie, Auf dem Hügel 69, D-53121 Bonn, Germany

Abstract. We investigate the relation between the Doppler factor determined from variations in total flux at 22 and 37 GHz, and the apparent transverse velocity determined from VLBA observations at 2 cm. The data are consistent with the relativistic beaming theory for compact radio sources, in that the distribution of $\beta_{\rm app}/\delta_{\rm var}$, for 30 quasars, is roughly consistent with a Monte Carlo simulation. The intrinsic temperature appears to be $\sim 2\times10^{10}$ K, close to the "equipartition value" calculated by Readhead (1994). We deduce the distribution of Lorentz factors for a group of 48 sources; the values range up to about $\gamma = 40$.

1. Introduction

Relativistic effects are commonly invoked to explain the superluminal motion and high brightness temperature ($T_{\rm b}$) seen in compact radio sources. $T_{\rm b}$ can be found from VLBI measurements or from variations in flux density; but these two methods depend differently on the Doppler factor. By measuring $T_{\rm b}$ in both ways, the Doppler factor and the Lorentz factor can be deduced, as well as $T_{\rm b}$(int), the intrinsic temperature in the synchrotron source. Lähteenmäki et al. (1999a) have done this for several sets of sources, and found that most of the $T_{\rm b}$(int) have a range around 10^{11} K. This is close to the "equipartition" value $\sim 5\times10^{10}$ K suggested by Readhead (1994), and the diamagnetic limit $\sim 3\times10^{11}$ K calculated by Singal (1986). It is at the bottom end of the range suggested by Kellermann & Pauliny-Toth for the limit due to the inverse-Compton catastrophe, $1-10\times10^{11}$ K. (See also Kellermann, these proceedings, page 185.)

In this paper we compare superluminal velocities, $\beta_{\rm app}$, with $\delta_{\rm var}$, the Doppler factor derived from variability. If a simple relativistic beaming theory is correct,

there will be a close connection between these two quantities. The new large and reliable sample of superluminal sources found in the VLBA 2 cm survey (Zensus et al., these proceedings, page 27) allows this to be done with some confidence, but see Section 6 for a discussion of the $\delta_{\rm var}$. We work with velocities from the VLBA 2 cm survey and Doppler factors from the Metsähovi flux density monitoring program at 22 and 37 GHz (Lähteenmäki & Valtaoja 1999b, hereafter LV99). We convert the Metsähovi values to our assumed cosmology, $H_\circ = 65\,{\rm km\,s^{-1}\,Mpc^{-1}}$, $\Omega_{\rm m} = 0.3$, $\Omega_\Lambda = 0.7$, but otherwise use the values found in their paper.

2. The Velocities

We only use velocities from the 2 cm survey which have three or more epochs of observation with an appropriately small error to the fit, and which satisfy several criteria for morphology. (Kellermann et al. 2003, in preparation.) The velocities are determined by a linear regression through the locations of the components being followed, and the errors shown in Figure 1 are the curve-fitting errors. We are using the *fastest* component for each source, on the grounds that their velocities should be representative of the true flow velocities. Slower-moving components, especially those at a bend in the jet, may be dominated by backward shock waves. Forward shock waves might also exist, and trying to understand their role is also a goal of the survey. Other geometries have been suggested for the jet, including a fast "spine" which we would preferentially see, surrounded by a slower shell. In this case, we think, the spine would also control the flux variations, so that using the fastest (spine) velocity for $\beta_{\rm app}$ is appropriate. In the next sections we assume that the pattern velocities are identical to the flow velocities; we comment on this assumption in Section 7.

Five sources in common to the $\delta_{\rm var}$ and $\beta_{\rm app}$ lists were excluded on the grounds that they only had components situated at a bend in the jet. We believe that in these cases we see a standing shock wave, or perhaps a stationary location in a helical jet where the flow is closest to the LOS, and hence boosted most strongly. In either case the measured velocity is a poor indicator of the flow velocity, and not useful in looking for relativistic effects. The final sample we use contains 48 sources: 4 galaxies, 14 BL Lacs, and 30 quasars.

3. The Doppler Factors

The 22 and 37 GHz light curves give the flux density in an outburst and the time constant Δt. As a model we take $c\Delta t$ to be the radius of an optically thick sphere. A solid angle is calculated and then the brightness temperature $T_{\rm b}$. (See Lähteenmäki et al. 1999a for details.) A further assumption is now needed, that the measured brightness temperature may be relativistically boosted above an intrinsic temperature $T_{\rm b}({\rm int})$. LV99 choose $T_{\rm b}({\rm int}) = 5 \times 10^{10}\,{\rm K}$, from the estimates of equilibrium temperature for a self-absorbed synchrotron source calculated by Readhead (1994). The variability Doppler factor is calculated as $\delta_{\rm var} = [T_{\rm b}({\rm var})/T_{\rm b}({\rm int})]^{1/3}$.

A more direct way to get the brightness temperature of a compact source is to measure its diameter and flux density with VLBI. The Doppler factor can then be calculated by reference to an assumed $T_{\rm b}$(int). In most cases of interest this yields a lower limit, because the cores of the sources are only slightly resolved with terrestrial interferometer baselines (Kellermann, these proceedings, page 185).

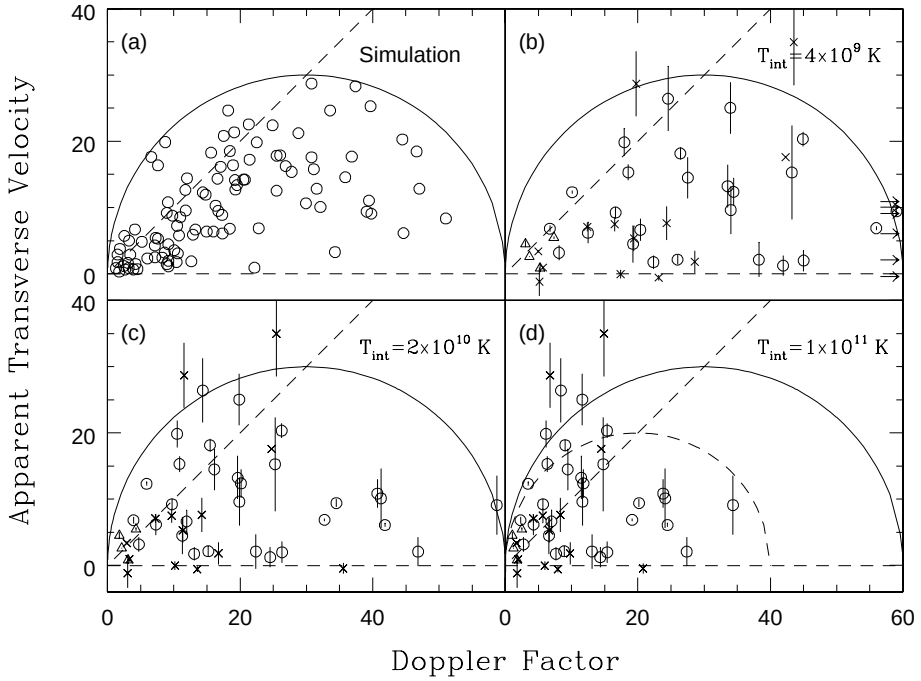

Figure 1. (a) Monte Carlo simulation of $(\beta_{\rm app}, \delta)$ for a flux-limited sample with N=100, $a = -1.25$. The diagonal line represents the "$1/\gamma$ cone", where the apparent velocity is maximized for a fixed γ. The semi-circle is the locus of points for $\gamma = 30$. (b) As in (a) with $\delta_{\rm var}$ calculated for $T_{\rm int} = 4 \times 10^9$ K. Circles: Quasars; Crosses: BL Lacs; Triangles: Galaxies. N=48 (c) As in (b) with $T_{\rm int} = 2 \times 10^{10}$ K. (d) As in (b) with $T_{\rm int} = 1 \times 10^{11}$ K. $\gamma = 20$ is shown as the dashed curve.

An alternative method of finding a Doppler factor involves the inverse Compton effect and the ratio of X-ray to radio flux. This method depends on knowing the diameter from VLBI, but is only weakly dependent on the X-ray flux, and so is close to the pure radio VLBI method described in the previous paragraph. A few cases have been studied in detail and give good results (e.g., Unwin et al. 1994).

4. The $(\beta_{\rm app}, \delta)$ Relation

Lister & Marscher (1997, hereafter LM97) have made Monte Carlo simulations of a flux-limited sample of compact sources drawn from a population that has a distribution of Lorentz factor $N(\gamma) \sim \gamma^a$. They assume flux boosting of the

form S$\sim \delta^2$, which is appropriate for the flat-spectrum core. Figure 1(a) shows a realization for $a = -1.25$. (See LM97 for a discussion of the exponents.) In this case the Lorentz factors are set such that $\gamma = 30$ is the maximum value in the sample, so the points all fall under the $\gamma = 30$ curve. Note that a majority of the sources lie under the diagonal line $\beta_{\rm app} = \delta$, or $\theta \approx 1/\gamma$, as they should, since the probability density for selecting a source peaks near $\theta = 1/2\gamma$ (Cohen 1989; Vermeulen & Cohen 1994, hereafter VC94; LM97). For a fixed γ, the apparent velocity is a maximum on this line.

In Figures 1(b), (c) and (d) we show values of $(\beta_{\rm app}, \delta_{\rm var})$ for our sample, for three values of $T_{\rm b}$(int). We believe that our data are representative of a flux-limited sample (Zensus et al., these proceedings, page 27), and LM97 show that $a = -1.25$ gives a reasonable fit to the apparent–velocity distribution of the Caltech-Jodrell flat spectrum survey (Taylor et al 1996). Hence our points should lie within a region bounded by a $\gamma =$ const curve, as in Figure 1(a). In Figure 1(b) 6 points are off scale on the x-axis, and the values of $\delta_{\rm var}$ go to 100. In Figure 1(d) we show two $\gamma =$ const curves, and it appears that, as in Figure 1(b), the points will not properly fill any γ=const curve. Figure 1(c) comes closest to the simulation, and, given the small number of points (30), it perhaps provides an adequate match. These comments about Figure 1 are confirmed by calculating the fraction f of sources inside the $1/\gamma$ cone. For the Monte Carlo simulation $f = 0.80$, and for the observations the values for the 30 quasars are (for increasing temperature) 0.87, 0.77, and 0.50. On this basis 1×10^{11} can be excluded, and 2×10^{10} is somewhat better than 4×10^9.

5. The distributions of $\beta_{\rm app}/\delta_{\rm var}$ and γ

The product $\gamma\theta$ is a useful quantity because the probability density function for θ depends only on $\gamma\theta$ for $\gamma^2 \gg 1$ (see VC94, Fig. 7). Hence the measured distribution of $\gamma\theta$ can be compared with a theoretical distribution, or one generated by a simulation, to see how closely the observations match the standard theory. In the previous section we found f, the fraction of sources with $\gamma\theta < 1$, and we picked $T_{\rm b}(\rm int) = 2 \times 10^{10}$ K because its value of f is close to the expected value. However, it is clear that looking at many values of $\gamma\theta$ would be more powerful than looking at f alone, as this would test the general distribution throughout the region below the $\gamma =$ const curves.

We actually use the ratio $\beta_{\rm app}/\delta_{\rm var}$, which, for $\gamma^2 \gg 1$, equals $\gamma\theta$. (A general result for a relativistic beam is $\beta_{\rm app} = \beta\gamma\delta \sin\theta$, where $\beta = v/c$.) We form the histogram of $\beta_{\rm app}/\delta_{\rm var}$, which counts the points between radii from the origin in Figure 1. In principle we can mix galaxies, BL Lacs, and quasars even though they have different parent populations, if we assume that a, and the slope of the luminosity function, are the same for all the populations. These assumptions seem somewhat dubious, however, and we only use the quasars.

Figure 2(a) shows the distribution of $\beta_{\rm app}/\delta_{\rm var}$ for the 100 sources in the simulation. Figures 2(b), (c), and (d) are for the 30 quasars, for the three values of $T_{\rm b}$(int). The histogram in Figure 2(d) is substantially flatter than that in 2(a) and supports our statement that $T_{\rm b}(\rm int) = 1 \times 10^{11}$ K is too high. In Figure 2(b) the distribution is too narrow, with a large spike in the first bin. This corresponds to the high values of $\delta_{\rm var}$ for this temperature. In Figure 2(c)

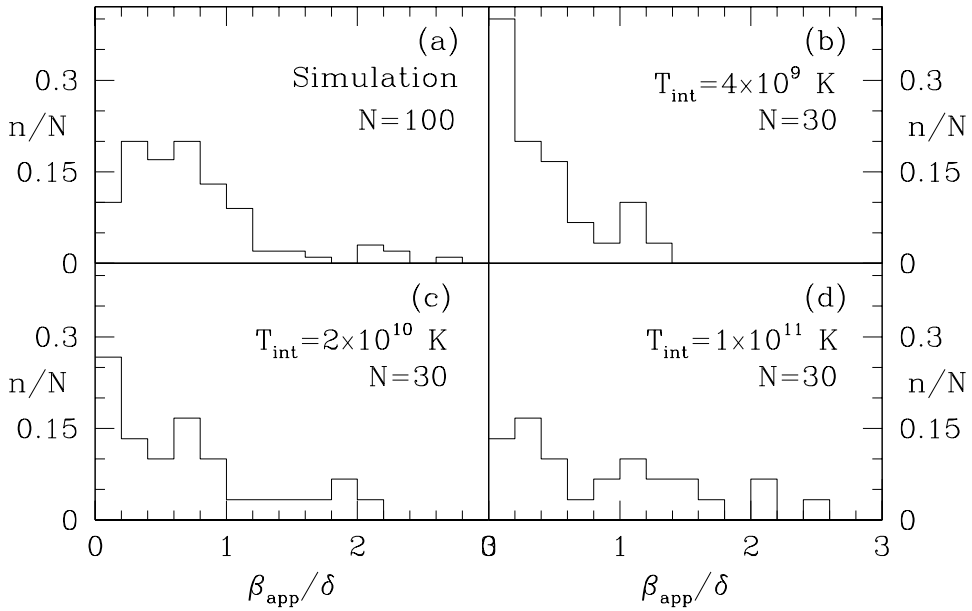

Figure 2. Histograms of $\beta_{\rm app}/\delta = \gamma\theta$. (a) Results from a Monte Carlo simulation, $N = 100$. (b), (c), and (d) Calculated for 30 quasars, with three different values of $T_{\rm b}$(int) used to calculate $\delta_{\rm var}$.

the histogram is a better match than the others, but it still has an excess in the first bin. We originally discarded 5 quasars because they had slow or stationary components located at a bend, and we believed that in those cases the measured velocity was not a good measure of the flow velocity. If we had kept those sources, they would have been in the first bin and the fit would be worse. In fact we discarded only the most egregious cases, and it is likely that there are other sources where we have measured a slow pattern rather than the flow velocity. This, we believe, explains at least part of the excess in the first bin.

The number of sources is too small to allow us to pick a particular "best" value for $T_{\rm b}$(int). However, it seems likely that for many quasars the intrinsic temperature in the compact synchrotron source is $1-3\times10^{10}$ K. For illustrative purposes below we use $T_{\rm b}$(int)$= 2\times10^{10}$ K, and we apply it to galaxies and BL Lacs as well as quasars.

We now calculate values of γ, using $T_{\rm b}$(int)$= 2\times10^{10}$ K. However, four BL Lacs have negative $\beta_{\rm app}$, with values within 1.5σ of zero. We assume that $\beta_{\rm app}+2\sigma$ is an upper limit to the velocity, and calculate the resulting upper limit to the Lorentz factor. The values of γ found in this way are nearly independent of how we pick $\beta_{\rm app}$, as can be seen from Figure 1; the $\gamma =$ const curves are vertical at $\beta_{\rm app} = 0$, where $\gamma = \delta_{\rm var}/2$. We could instead adopt a lower limit and assume that the negative sources are in the forward jet, but moving towards the center. In this case their flux would be de-boosted, whereas in fact they are strong sources. Alternately, we could assume that they are inward-moving in the back jet. We reject this because there is plentiful evidence that in these compact sources we see only forward jets.

Figure 3 shows the distribution of Lorentz factor for the 48 sources, with upper limits denoted by arrows. The quasars have a broad distribution between 5 and 25, with a few quasars both higher and lower. The galaxies and most of the BL Lacs have $\gamma < 10$. However, the two highest γ have large error bars (the two BL Lacs above the curves in Fig. 1) and they are not reliable. The quasars and BL Lacs have a wide distribution of γ, but there are insufficient data to see if they might match any of the distributions found in the Monte Carlo simulations by LM97. We note that some of their distributions for γ have a minimum in the first bin, as in Figure 3. It is interesting to note that Homan (these proceedings, page 35) has estimated γ for the source 3C 279, by analyzing a change in velocity, and assuming that it is due to a change in θ, not γ. He finds $\gamma \gtrsim 15$. Our calculation using $\delta_{\rm var}$ and $\beta_{\rm app}$ gives $\gamma = 19$, for $T_{\rm b}({\rm int}) = 2 \times 10^{10}$ K. These methods of finding γ are largely independent. Their good agreement adds to our conclusion that for many sources the intrinsic temperature is $\sim 1 - 3 \times 10^{10}$ K.

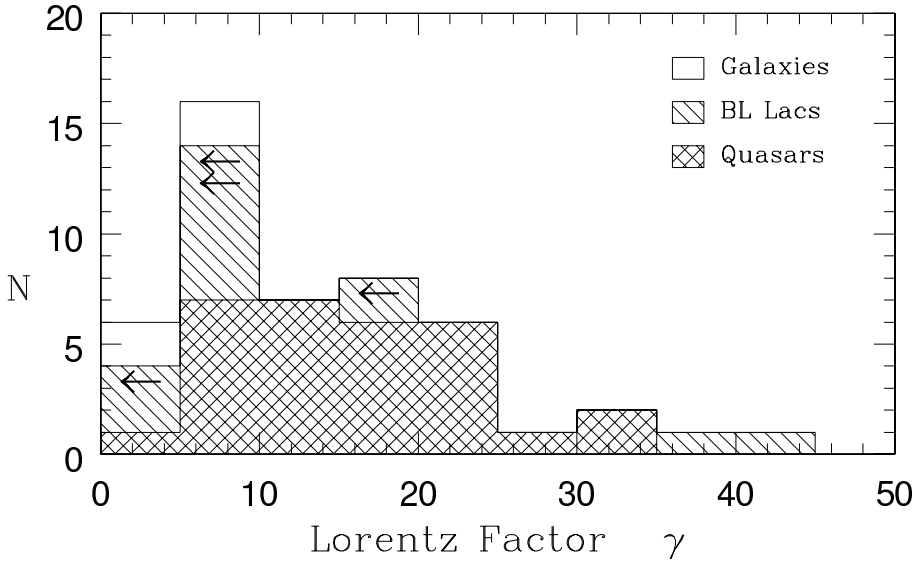

Figure 3. Histogram of Lorentz factors, calculated from $\beta_{\rm app}$ and $\delta_{\rm var}$ based on $T_{\rm int} = 2 \times 10^{10}$ K. Arrows indicate upper limits. $N = 48$

6. Reliability of $\delta_{\rm var}$

We have several concerns over the reliability of the $\delta_{\rm var}$ values. The first involves the procedure used to calculate $\delta_{\rm var}$ from a light curve. To partially address this we made some independent determinations of $\delta_{\rm var}$ using the same procedures as Lähteenmäki et al. (1999), and Valtaoja, et al. (1999). We used the 8 and 15 GHz variability curves from the University of Michigan web site, and the 22 and 37 GHz data from the Metsähovi web site. We found that the higher-frequencies gave better results, because there was less blending between outbursts. We did not try to investigate the effect of non-overlap of the epochs of the $\delta_{\rm var}$ and $\beta_{\rm app}$

measurements; but we have seen that for most sources successsive outbursts have a similar velocity. Also, Valtaoja et al. (1999) state that the apparent brightness temperature of well-defined flares does not vary much in any one source. However, the most important factor appears to be the identification of individual outbursts, even at the highest frequencies. This identification is somewhat subjective, and apparently we were more conservative and our values for $\delta_{\rm var}$ were consistently about 30% lower than the values published by LV99. In a few cases there were larger discrepancies, apparently caused by our missing some large flares not yet posted on the Metsähovi web site (Valtaoja, private communication). Thus we think that this systematic effect might limit the accuracy of $\delta_{\rm var}$ to about 30%.

The second general concern involves the model used for the source. The calculation simply assumes that the time constant of the flare is related to a radius by $r = c\Delta t$, and then that the solid angle of the source is $\Omega = \pi(r/D)^2$, where D is the metric distance to the source. If we were to assume instead that the diameter, not the radius, is given by $c\Delta t$, then the $T_{\rm b}$(int) would have to be increased by a factor of 4 to reproduce the simulation in Figure 1(a). Actually, $c\Delta t$ should be regarded as an upper limit to r; this might further increase $T_{\rm b}$(int). Furthermore, to be more realistic, the sphere should be replaced by a shock wave. See e.g., Marscher & Gear (1985).

7. Pattern and Flow Velocities

In this work we have assumed that the pattern velocity we measure with the VLBA is the same as the flow velocity of the beam. However it is clear that this is not always so. For example, we eliminated several cases where the pattern is stationary at a bend in the jet, on the grounds that the bright spot is due to a standing shock wave, and its zero motion is not representative of the flow velocity.

VC94 made a simple model to study differing pattern and flow velocities; namely, that the flow and the pattern have different γ, and their ratio $r = \gamma_{\rm p}/\gamma_{\rm b}$ has a characteristic value. From the early VLBI data they showed that if $r = 1$ in all sources, then γ cannot be constant, and vice versa. From Figure 3 it is quite clear that γ is not constant in the compact sources. That does not mean that r is constant; indeed, since we count stationary sources as having $r = 0$, then r has some distribution also. If the distribution of r mostly has values below unity, then in Figure 1 $\beta_{\rm app}$ must be increased. The distribution of γ will shift to higher values, and its shape may change. It is difficult to predict whether the best-matching $T_{\rm b}$(int) will increase or decrease, as that depends on the details of the r distribution.

8. Conclusions

We have combined variability Doppler factors with superluminal motions, for a sample of about 50 radio sources. The distribution of $\beta_{\rm app}/\delta_{\rm var}$ is roughly similar to that found in a Monte Carlo simulation, provided the intrinsic temperature in the synchrotron-emitting medium is $T_{\rm b}$(int)$\sim 2 \times 10^{10}$ K. This is near the "equipartition temperature", $\sim 5 \times 10^{10}$ K suggested by Readhead (1994). It

is below the upper limit based on the inverse-Compton effect, $1 - 10 \times 10^{11}$ (Kellermann & Pauliny-Toth 1969; Kellermann, these proceedings, page 185), and the diamagnetic limit calculated by Singal (1986), $\sim 3 \times 10^{11}$ K.

The galaxies, and most of the BL Lacs, have $\gamma < 10$, when calculated with $T_{\rm b}({\rm int}) = 2 \times 10^{10}$ K. The quasars have a distribution which is flat between $\gamma = 5$ and $\gamma = 25$, with only a few quasars above and below these limits.

We are indebted to H. Aller, M. Aller, M. Kadler, and E. Valtaoja for helpful discussions. The NRAO and the VLBA are operated by AUI, under cooperative agreement with the NSF. This research has made use of data from the University of Michigan Radio Astronomy Observatory which is supported by funds from the University of Michigan.

References

Cohen, M. H. 1989, in BL Lac Objects, ed. L. Maraschi, T. Maccacaro, & M.-H. Ulrich, Lecture Notes in Phys. Vol. 334, (Berlin: Springer), 13

Kellermann, K. I., et al. 1998, ApJ, 115, 1295

Kellermann, K. I., & Pauliny-Toth, I. I. K. 1969, ApJ, 155, L71

Lähteenmäki, A., Valtaoja, E., & Wiik, K. 1999a, ApJ, 511, 112

Lähteenmäki, A., & Valtaoja, E. 1999b, ApJ, 521, 493 (LV99)

Lister, M. L., & Marscher, A. P. 1997, ApJ, 476, 572 (LM97)

Marscher, A. P. & Gear, W. K. 1985, ApJ, 298, 114

Readhead, A. C. S. 1994, ApJ, 426, 51

Singal, A. K. 1986, A&A, 155, 242

Unwin, S. C., et al. 1994, ApJ, 432, 103

Taylor, G. B., et al. 1996, ApJS, 107, 37

Valtaoja, E., et al. 1999, ApJS, 120, 95

Vermeulen, R. C., & Cohen, M. H. 1994, ApJ, 430, 467 (VC94)

Zensus, J. A., et al. 2002, AJ, 124, 662